Rangeland Ecology & Management xxx (xxxx) xxx–xxx

Contents lists available at ScienceDirect

Rangeland Ecology & Management

journal homepage: http://www.elsevier.com/locate/rama

Original Research

Validating a Time Series of Annual Grass Percent Cover in the Sagebrush Ecosystem☆

Stephen P. Boyte [a,*], Bruce K. Wylie [b], Donald J. Major [c]

[a] Senior Scientist, Stinger Ghaffarian Technologies, contractor to the US Geological Survey (USGS) Earth Resources Observation and Science (EROS) Center, Sioux Falls, SD 57198, USA
[b] Research Physical Scientist, USGS EROS Center, Sioux Falls, SD 57198, USA
[c] Fire and Landscape Ecologist, Bureau of Land Management, Boise, ID 83709, USA

ARTICLE INFO

Article history:
Received 25 April 2018
Received in revised form 28 August 2018
Accepted 13 September 2018
Available online xxxx

Key Words:
Assessment Inventory and Monitoring (AIM) data
Bromus tectorum
ecological model
invasive annual grass
Moderate Resolution Imaging Spectroradiometer (MODIS)
sagebrush

ABSTRACT

We mapped yearly (2000–2016) estimates of annual grass percent cover for much of the sagebrush ecosystem of the western United States using remotely sensed, climate, and geophysical data in regression-tree models. Annual grasses senesce and cure by early summer and then become beds of fine fuel that easily ignite and spread fire through rangeland systems. Our annual maps estimate the extent of these fuels and can serve as a tool to assist land managers and scientists in understanding the ecosystem's response to weather variations, disturbances, and management. Validating the time series of annual maps is important for determining the usefulness of the data. To validate these maps, we compare Bureau of Land Management Assessment Inventory and Monitoring (AIM) data to mapped estimates and use a leave-one-out spatial assessment technique that is effective for validating maps that cover broad geographical extents. We hypothesize that the time series of annual maps exhibits high spatiotemporal variability because precipitation is highly variable in arid and semiarid environments where sagebrush is native, and invasive annual grasses respond to precipitation. The remotely sensed data that help drive our regression-tree model effectively measures annual grasses' response to precipitation. The mean absolute error (MAE) rate varied depending on the validation data and technique used for comparison. The AIM plot data and our maps had substantial spatial incongruence, but despite this, the MAE rate for the assessment equaled 12.62%. The leave-one-out accuracy assessment had an MAE of 8.43%. We quantified bias, and bias was more substantial at higher percent cover. These annual maps can help management identify actions that may alleviate the current cycle of invasive grasses because it enables the assessment of the variability of annual grass — percent cover distribution through space and time, as part of dynamic systems rather than static systems.

Introduction

Annual grass percent cover in the sagebrush ecosystem is highly variable both interannually and spatially. After these grasses complete their lifecycles each year, they become highly flammable and create beds of fine fuel capable of spreading fire (Whisenant, 1990; Balch et al., 2013). Because of the spatial and temporal variability of annual grasses, the annual extent and potential impact of these beds of fuel over large geographic areas are unknown without yearly maps that estimate annual grass percent cover. We developed a satellite-based time series (2000–2016) of maps that estimate annual grass percent cover in the sagebrush ecosystem of the western United States and identify the extent of these beds of fuel. These maps can serve as a tool that helps land managers and scientists understand the ecosystem's response to weather variations, disturbances, and management in the context of annual grass variability. This understanding can occur because annual grasses are positively correlated with precipitation (Bradley and Mustard, 2005; Pilliod et al., 2017), and the combined effect of fire and grazing leads to reduced resistance to annual grass invasion through altered dynamics of other biotic factors (Condon and Pyke, 2018). As annual grass extents expand in sagebrush ecosystems, the associated biodiversity loss and continuity of fine fuels results in grass-fire cycles (Brooks et al., 2004) that increase the threat to adjacent sagebrush communities, increase the danger to human-built structures, reduce air quality, and compromise grazing and recreational resources. This new fire regime induces the replacement of native plant species with invasive plants (D'Antonio and Vitousek, 1992; D'Antonio, 2000; Brooks et al., 2004), which causes the displacement of wildlife species, reducing their populations (Connelly et al., 2011). In the past 30 yr, wildfires have caused more widespread damage in western ecosystems than occurred

☆ Any use of trade, firm or product names is for descriptive purposes only and does not imply endorsement by the US government. Research was funded by the Great Basin Landscape Conservation Cooperative, Bureau of Land Management, and US Geological Survey Land Change Science program. The authors declare no competing interests. Work was performed under USGS contract G15PC00012 (Boyte).

* Correspondence: Stephen P. Boyte, Stinger Ghaffarian Technologies, 47914 252nd St, Sioux Falls, SD 57198, USA. Tel.: +1 605 594 6171.
E-mail address: sboyte@contractor.usgs.gov (S.P. Boyte).

https://doi.org/10.1016/j.rama.2018.09.004
1550-7424/

under the historical fire regime (Connelly et al., 2011; Schoennagel et al., 2017). Balch et al. (2013) determined that fire frequency, size, and duration have increased substantially in areas infested with cheatgrass, a dominant invasive annual grass in the sagebrush ecosystem. With climate change and climate-driven vegetation change playing important roles in the potential transformation of fire regimes (Liu and Wimberly, 2016), the lengthening of the fire season in the western United States is likely. Kerns and Day (2017) discovered that in experimental plots in the Blue Mountains ecoregion within the Malheur National Forest, Oregon, autumn burns led to higher cover of cheatgrass than areas that experience no burns (controls) or spring burns. These findings make knowledge of the extent and magnitude of the annual grass invasion essential, both its interannual and spatial variabilities, especially as endogenous and exogenous influences change. Therefore, while validating the accuracy of a time series of annual grass − percent cover maps with ground-truth data can be problematic, the validation is important for determining data limitations.

In this study, we used 7-day best pixel composites of enhanced Moderate Resolution Imaging Spectroradiometer (eMODIS) normalized difference vegetation index (NDVI) data that were available weekly (the eMODIS NDVI data are described in more detail in the Methods section and can be downloaded at https://earthexplorer.usgs.gov/). Consistent and frequent acquisitions of spatially explicit remotely sensed data can mitigate some challenges of using remotely sensed data (Jenkerson et al., 2010; French et al., 2013) and be used to build time series datasets that allow monitoring of many diverse phenomena. eMODIS NDVI senses relatively quick-changing ecological processes (Wylie et al., 2012; Browning et al., 2015) and has done so over long periods at relatively low cost because of its fine-scale temporal acquisition schedule, use of data from a long-flying satellite, and broad coverage. eMODIS NDVI data can also be used to measure the variability of annual vegetation's response to weather, disturbances, and/or management (Wylie et al., 2012). Maynard et al. (2016) discovered that in a time series (2000–2012), MODIS NDVI predicted vegetation biomass better than Landsat 5 largely due to MODIS's high temporal resolution composites. A time series of remotely sensed data is valuable, in part, because it allows the establishment of an average value for each mapped unit. Comparisons between that average and its time series can elicit valuable information when one or more periods deviate substantially from normal (Boyte et al., 2018).

Remotely sensed − based ecological modeling projects generally rely on field data or its derivatives, and field data are generally difficult and expensive to obtain and a challenge to directly associate with remotely sensed − based results (Bradley et al., 2018). Validating a time series of ecologically and remotely sensed − based results with field-based datasets can be problematic for at least two reasons. First, independent field data are scarce and may not exist in a study area for all, or even some, years in a time series (Browning et al., 2015). Second, the spatial resolution of the remotely sensed data and the spatial representation of field plots may be incongruent and require either the spatial manipulation of one dataset to match the other or the acceptance of spatial resolution differences between datasets. Either of these circumstances influence validation efforts when comparing satellite data with field data. When conducting remotely sensed ecological studies in sagebrush ecosystems, the problems of spatial incongruence between the remotely sensed data and the field plots can be exacerbated (Maynard et al., 2016) because, in their native states, these ecosystems can have highly heterogeneous vegetation patterns with areas of substantial bare ground that produce mixed satellite reflectance signals. Therefore, the larger the spatial footprint of the individual pixels in the remotely sensed data, the more likely the differences will be substantial between the remotely sensed data and the field data (Browning et al., 2017).

The goals of this study are twofold: 1) contribute to the understanding of the historical annual grass invasion in the sagebrush ecosystem and 2) visually demonstrate the spatial and interannual variability of annual grass percent cover in this study's time series. In the process of reaching these two goals, we accomplish three objectives: 1) develop a time series (2000–2016) of yearly maps that describe the relative abundance and extent of annual grass percent cover in the sagebrush ecosystem; 2) describe and illustrate the annual grass − percent cover mapping model and its results; and 3) report the relative accuracy of this time series. Within the context of these objectives, we hypothesize that, in already invaded areas, the interannual variability in the time series of maps will closely follow seasonal precipitation patterns and the overall accuracy of the maps will show a mean absolute error (MAE) rate of < 10%. We establish these hypotheses on the basis of our understanding of previous work that describes cheatgrass response to highly variable precipitation (Bradley and Mustard, 2005; Pilliod et al., 2017) and drivers of environmental resistance to exotic brome grasses (i.e., cheatgrass [*Bromus tectorum* L.] and red brome [*Bromus rubens* L.]), such as elevation and soil moisture and temperature regimes (Chambers et al., 2016).

Methods

Study Area

The study area encompassed about 1.3 million km^2 of the western United States, including all of Wyoming and parts of 10 other states (Fig. 1). All or part of 20 ecoregions fell within the study area's boundary, including all of the Northern Basin and Range, the Central Basin and Range, and the Snake River Plain (Commission for Environmental Cooperation, 2009). This study focused on land dominated by shrub and grassland/herbaceous vegetation (National Land Cover Database ([NLCD], http://www.mrlc.gov/nlcd2001.php) at or below 2 250-m elevation, and this included approximately 52.5% of the mapped area. A mask covered the other 47.5% of the area. In previous work, we mapped average cheatgrass percent cover at < 2% at an elevational range of 1 750 − 2 000 m (Boyte et al., 2015b, 2016). Consequently, we set a 2 250-m threshold to focus our study on likely areas of annual grass invasion while allowing for expansion of the future annual grass envelope. The study area's 30-yr (1981 − 2010) average precipitation equaled 416 mm with a range from 46 mm in the lower, drier areas to 2 890 mm on higher peaks. The 30-yr temperature averages ranged from −0.38° C to 14° C (PRISM Climate Group, http://prism.oregonstate.edu). Elevations ranged from −72 m to 4 357 m with a mean of 1 818 m (North American Vertical Datum of 1988). Much of the area was a shrub steppe environment that historically was dominated by sagebrush (*Artemisia* spp.). The sagebrush coexisted with perennial grasses like bluebunch wheatgrass (*Pseudoroegneria spicata* [Pursh] A. Love), Idaho fescue (*Festuca idahoensis* Elmer), and Sandberg bluegrass (*Poa secunda* J. Presl) and annual invasive grasses like cheatgrass (*Bromus tectorum* L.), ventenata (*Ventenata dubia* [Leers] Coss.), annual red brome (*Bromus reubens* L.), and medusahead (*Taeniatherum caput-medusae [L.] Nevski*) (West and Young, 2000). Other common woody species included rabbitbrush (*Chrysothamnus* Nutt.), winterfat (*Krascheninnikovia* Guldenstaedt), greasewood (*Sarcobatus* Nees), shadscale (*Atriplex confertifolia* [Torr, & Frem] S. Watson), and fourwing saltbush (*Atriplex canescens* [Pursh] Nutt.) (Wiken et al., 2011). Other herbaceous species included Thurber's needlegrass (*Achnatherum thurberianum* [Piper] Barkworth), squirreltail (*Elymus elymoides* [Raf.] Swezey), western wheatgrass (*Pascopyrum smithii* [Rydb.] A. Love), and needle and thread (*Hesperostipa* [Elias] Barkworth) (Wiken et al., 2011).

Data

Dependent Variables

We accessed three spatially explicit datasets with 30-m spatial resolution as reference data. This included a north-central Nevada cheatgrass percent cover dataset (~2001) and an Owyhee Upland annual

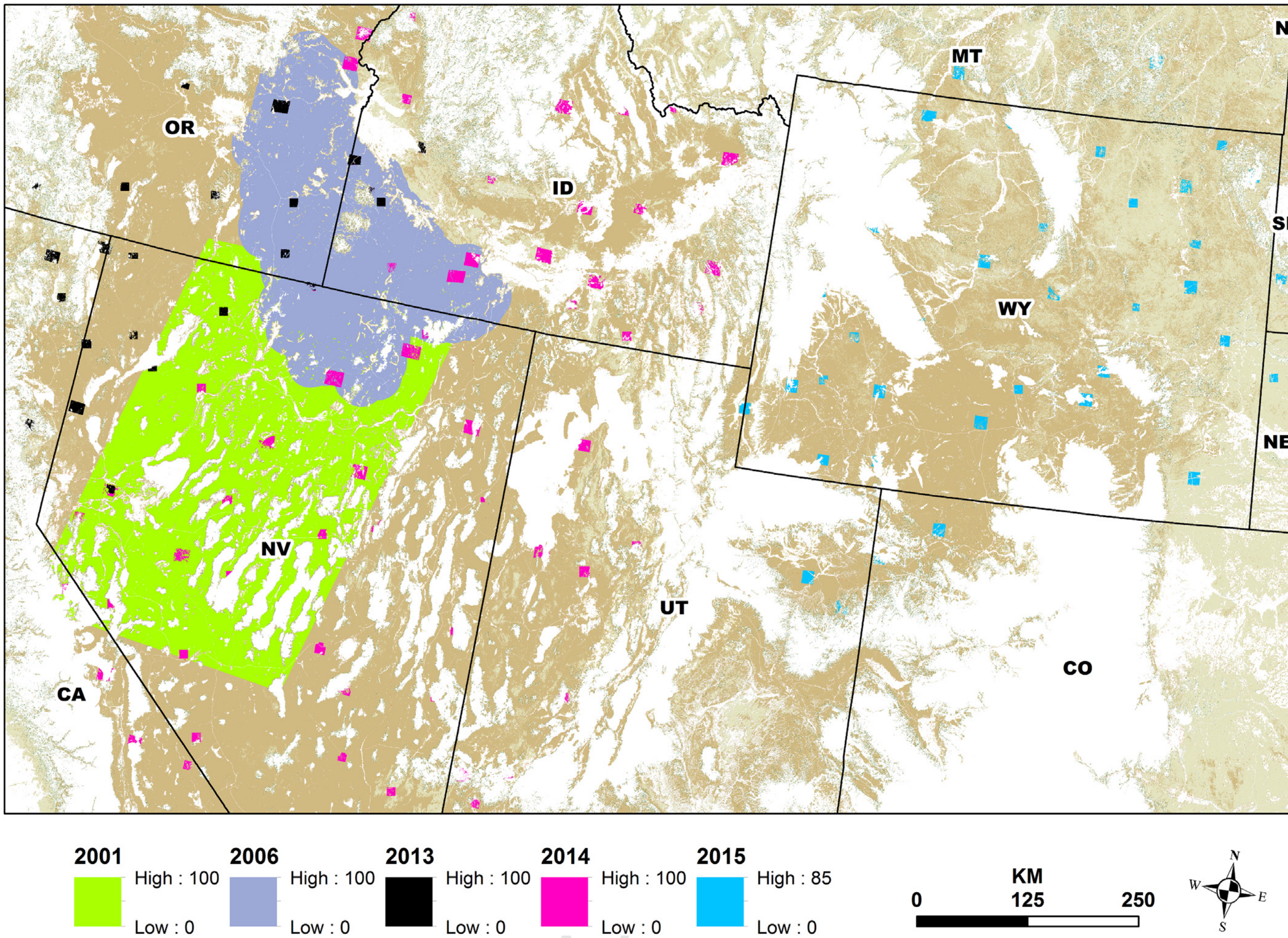

Figure 1. The study area showing the general spatial distribution of training data locations. Each location is colored based on the yr the training data represent. Multiple pixels reside within each location, but every potential pixel is not selected as a training point. The values associated with each yr show that yr's training data percent cover range. We harvested training data only from locations classified by the National Land Cover Database (NLCD) as shrub or grassland/herbaceous and at or below 2 250 m elevation. A mask (white) covers all other areas. The size and shape of each training data location varies on the basis of the pixels within that location that meet the NLCD and elevation parameters. The 2011 NLCD serves as a backdrop.

grass index (2006) (Nevada Natural Heritage Program, http://heritage.nv.gov/). We also used percent cover estimates of annual herbaceous vegetation (2013–2015) datasets. These datasets used WorldView data and were developed by a team of researchers, field technicians, and Global Information System/remote sensing experts associated with the US Geological Survey (USGS) NLCD project (Xian et al., 2015). Because we utilized reference datasets from sources that quantify cheatgrass, annual grass, and annual herbaceous vegetation we refer to the data this study produced as annual grass — percent cover maps. We used the cheatgrass and annual grass datasets in two previous publications (Boyte et al., 2015a, 2016) where we described the datasets and their accuracy. In brief, these two datasets were developed using 2001 Landsat 7 Enhanced Thematic Mapper Plus (ETM+) or 2006 Landsat 5 Thematic Mapper (TM) satellite data combined with geophysical variables along with data from more than 650 field plots (Peterson, 2005, 2007). The 2001 cheatgrass dataset experienced a correlation coefficient (r) of 71% and a root mean squared error (RMSE) of 9.1% (Peterson, 2005). The 2006 annual grass dataset had an RMSE between 10% and 16%, with 75% of field plots within 14% of the field measurements (Peterson, 2007). The annual herbaceous datasets were developed using a multi-scaling approach that integrated sample data from field plots with high-resolution (~2 m) WorldView-2 and WorldView-3 satellite data with 8 spectral bands (Xian et al., 2015). Algorithms that predict annual herbaceous percent cover were developed with rule-based regression-tree software, and then the algorithms were applied to a mapping application that generated 2-m spatially explicit estimates. The 2-m estimates were spatially averaged to a 30-m spatial resolution using the degrade tool in ERDAS Imagine. This tool averages the original pixels that compose the new, larger spatial resolution pixels. These 30-m datasets were then, as were the 30-m cheatgrass percent cover and annual grass index data, spatially averaged using a 7 × 7 focal mean and resampled to 250-m to match the spatial resolution of the eMODIS NDVI data.

Independent Variables

Independent variables were chosen that help quantify annual grass percent cover. These variables had to be spatially explicit and cover the entirety of the study area. They included satellite, topographic, soils, climatic, land cover, and disturbance datasets. The satellite data were generated from 17 yr (2000–2016) of 250-m eMODIS NDVI data and used to develop four derivative variables for each year: mean growing season NDVI (Spring GSNs), mean summer NDVI (Summer GSNs), annual grass indices, and estimated start of season spring growth. The NDVI product used the MODIS red (620–670 nm) and near-infrared (NIR) (841–876 nm) bands in an equation (Eq. (1)) (Jensen, 2005) that measures dynamic vegetation greenness. The eMODIS NDVI data consisted of 7-d best pixel composites derived from daily data where a minimum-value-composite algorithm identified the best pixel in each 7-d period by filtering through input surface reflectance of poor quality, negative values, low view angles, clouds, and snow cover

Please cite this article as: Boyte, S.P., et al., Validating a Time Series of Annual Grass Percent Cover in the Sagebrush Ecosystem, (2018), https://doi.org/10.1016/j.rama.2018.09.004

(Jenkerson et al., 2010). These composites mitigated problems caused by clouds, shadows, off-nadir fields of view, and atmospheric effects (Jenkerson et al., 2010). After acquisition, the composites were temporally smoothed to further mitigate residual cloud effects. The 7-d temporal resolution of the eMODIS NDVI data captured the phenological dynamics of rapidly developing annual grasses and, when combined with this data source's ability to mitigate problems inherent to remotely sensed data, made it a strong choice to monitor annual grass percent cover on an annual time step.

$$NDVI = \frac{\rho_{nir} - \rho_{red}}{\rho_{nir} + \rho_{red}}, \text{where} \begin{cases} \rho_{red=red\ reflectance} \\ \rho_{nir=near\ infrared\ reflectance} \end{cases} \qquad (1)$$

The annual grass indices were a function of Spring GSNs and Summer GSNs (Eq. (2)) (Kokaly, 2011). Each variable was spatially and temporally dynamic and reflected the variation in weather, disturbances, management, and site characteristics at each pixel. The start of season spring growth was a phenologically driven variable used only to identify each pixel's dynamic starting point (the eMODIS NDVI weekly composite) of Spring GSN's integration period (Boyte et al., 2015b). We incorporated an independently developed 250-m remotely sensed phenology dataset derived from eMODIS NDVI, start of season time (SOST) (http://phenology.cr.usgs.gov/index.php), into the model as an independent variable. To account for fire disturbances in our model, we included a 250-m time-since-fire dataset that used Monitoring Trends in Burn Severity data (https://www.mtbs.gov/). Elevation data and their derivatives, steep slope with aspect and a compound topographic index, were produced from 30-m data available from The National Map (https://nationalmap.gov/elevation.html). Slopes exceeding 8.5% were classified as steep. North-facing and south-facing slopes were defined by azimuths from 315 degrees to 45 degrees and 135 degrees to 225 degrees, respectively. Digital soils data included 30-m available water capacity and soil organic matter from the POLARIS website (http://stream.princeton.edu/POLARIS/). To define precipitation zones in our study area, we resampled 30-yr averages (1981–2010) of PRISM (http://prism.oregonstate.edu) precipitation data at 800 m spatial resolution to 250 m using bilinear interpolation. We used one categorical dataset, the 30-m 2011 National Land Cover Database, to help stratify the model at areas classified as shrub or herbaceous. We spatially averaged all 30-m datasets and then resampled them to 250 m to match the eMODIS NDVI data.

$$\text{Annual Grass Index} = \frac{\text{SpringGSN} - \text{Summer GSN}}{\text{Spring GSN} + \text{Summer GSN}}, \qquad (2)$$
$$\text{where} \begin{cases} \text{Spring GSN} = \text{integrated growing season NDVI} \\ \text{Summer GSN} = \text{integrated summer NDVI} \end{cases}$$

Developing the Rule-Based Regression-Tree Model

The dependent and independent variables described earlier provided information on training cases for our model. We entered these variables into rule-based, regression-tree software (https://www.rulequest.com/) and used them to develop a spatially explicit model of annual grass—percent cover estimates. The regression-tree software stratified rules by relating the dependent variable to the independent variables. Each rule had an associated algorithm that was used to develop an estimation for all pixels that fit that specific rule. We reduced the number of rules and removed some variables from our model (Table 1). The fewer rules employed by the model, the more generalized the model estimates. The more rules employed by the model, the more specific the model estimates, and the more likely the model would be overfit (Gu et al., 2016). More rules could also have added intermittent spatial artifacts to mapping outputs, artifacts that reflect the spatial pattern of specific independent variables and not what was on the ground. Some modelers remove independent variables that add spatial artifacts to their maps. We tested the number of model rules at multiple values between 100 and 25, and we found that 27 rules optimized the model relatively well and left its mapping outputs mostly free of spatial artifacts. We trained the annual grass model on 33 746 randomly stratified points that were spaced through time (Table 2) and spatially distributed throughout the unmasked portion of the study area (see Fig. 1) where herbaceous/grasslands or shrub lands were the dominant land cover (http://www.mrlc.gov/nlcd2001.php). We harvested the training points from the 5 yr of data described in the dependent variables subsection and built a model robust to dynamic conditions like weather, disturbances, and management. Training a synoptic model with points that represented a variety of conditions encountered through time and space reduced model extrapolation and created better model estimates (Jung et al., 2009; Gu et al., 2012).

Table 1
Driving variables for the annual grass—percent cover model. Frequency (%) of use is shown for each variable used to establish rule conditions and the associated linear regression models. Dashes indicate that a variable was not used. The model was constructed of 5 committees and 27 rules.

Driving variable	Rule conditions	Linear regression model
Spring GSN	78	95
Elevation	78	93
Available water capacity	50	69
30-yr precipitation	45	77
Start of season time	33	73
Annual grass index	16	68
Time since fire	15	41
National land cover database	13	–
Soil organic matter	11	77
Summer GSN	9	93
Compound topographic index	–	35
South facing steep slope	–	14
North facing steep slope	–	13

Based on 9 randomizations: training data $R^2 = 0.76$. Mean absolute error = 5.79 ± 0.03. Test data $R^2 = 0.74$. Mean absolute error = 5.84 ± 0.11. Ten-fold cross validation $R^2 = 0.74$. Several variables were initially applied to the model but omitted because they caused excessive spatial artifacts in the maps. These variables include a latitude proxy, Major Land Resource Area, LANDFIRE environmental site potential, 30-yr temperature maximums, and 30-yr temperature minimums.

Developing the Time Series of Annual Grass Maps

The model developed by the regression-tree software for the annual grass estimates was applied using a mapping application, MapCubist. USGS Earth Resources Observation and Science (EROS) Center computer scientists developed MapCubist using publicly available source code provided by RuleQuest (https://www.rulequest.com/). This code used GDAL (http://www.gdal.org/), an open-source raster processing library to produce an application capable of reading a list of rasters, applying the rule-based, linear regression equations to the independent variables and producing output estimates for each year in the time series. All rasters of independent variables represented the entire study area extent.

Table 2
The number of training points by yr.

Yr	Points
2001	4804
2006	4418
2013	4970
2014	10061
2015	9493

Please cite this article as: Boyte, S.P., et al., Validating a Time Series of Annual Grass Percent Cover in the Sagebrush Ecosystem, (2018), https://doi.org/10.1016/j.rama.2018.09.004

Model Evaluation

The regression-tree software produced model estimates based on the associations between the dependent and independent variables and generated model accuracy metrics. These metrics included the correlation coefficient and an MAE rate. Several user-controlled parameters changed the model structure, and these parameters included the number of committee models used iteratively to improve substantially incorrect estimates, percentage of model extrapolation allowed, and maximum number of rules the model used to stratify the data. Once we optimized the model's parameters (Gu et al., 2016), we set the regression-tree software to begin with a random seed and then conducted nine bootstrap model runs. We averaged the accuracy metrics of the nine model runs for overall model accuracy. Separately, we generated a model with a 10-fold cross validation where each of the 10 folds was withheld sequentially as test data. This validation process also output a correlation coefficient and an MAE rate. We converted the correlation coefficient to an R^2.

Assessment Inventory and Monitoring Data

We downloaded several yr (2011–2016) of Bureau of Land Management (BLM) Assessment Inventory and Monitoring (AIM) data that coincided with our study period and area (https://gis.blm.gov/AIMdownload/layerpackages/BLM_AIM_Terrestrial.lpk) (Fig. 2). AIM data are designed "to quantitatively assess the condition, trends, amount, location, and spatial pattern of natural resources on the nation's public lands" (https://landscape.blm.gov/geoportal/catalog/AIM/AIM.page). Herrick et al. (2017) described the collection of AIM data where a line-point intercept method was used with a pin to measure vegetation percent cover and composition. Plot transect lengths typically extended from 25 to 50 m, and plot designs took several forms including a spoke, parallel lines, or a single straight or curved line. We compared the AIM data to our mapping estimates, calculated the correlation coefficient, MAE rate, and normalized root mean square error (nRMSE) for each individual year and for all years combined (Table 3). The nRMSE is a dimensionless statistic that measures model fit with no regard for a dataset's range and allows comparison between multiple RMSE calculations (Homer et al., 2012). Two incongruities exist between the AIM data and the mapped estimates of annual grass percent cover. First, the AIM process uses an "any hit" technique—any time a pin is dropped, every plant the pin touches is recorded as a hit and included in the percent cover calculation, irrespective of whether the hit is in the upper or lower canopy. This can result in vegetation cover hypothetically being recorded at > 100%. Passive radiometers (visible, infrared, and shortwave infrared) on satellites respond primarily to the characteristics of the top canopy layers with low or no sensitivity to the lower canopy levels in dense vegetation. Mapped estimates did not exceed 100%. Second, and likely more important, spatial resolution differences existed between the AIM data and mapped estimates, which is a common problem when validating remote sensing data (Bradley et al., 2018). Spatially, the AIM-transect plots represented approximately $4.5-15.2\%$ of a 250-m pixel (a 250-m pixel represents 6.25 ha, so AIM-transect plots represent $\approx 0.28-0.95$ ha), depending on transect lengths in the plot design. Consequently, in many cases, AIM annual

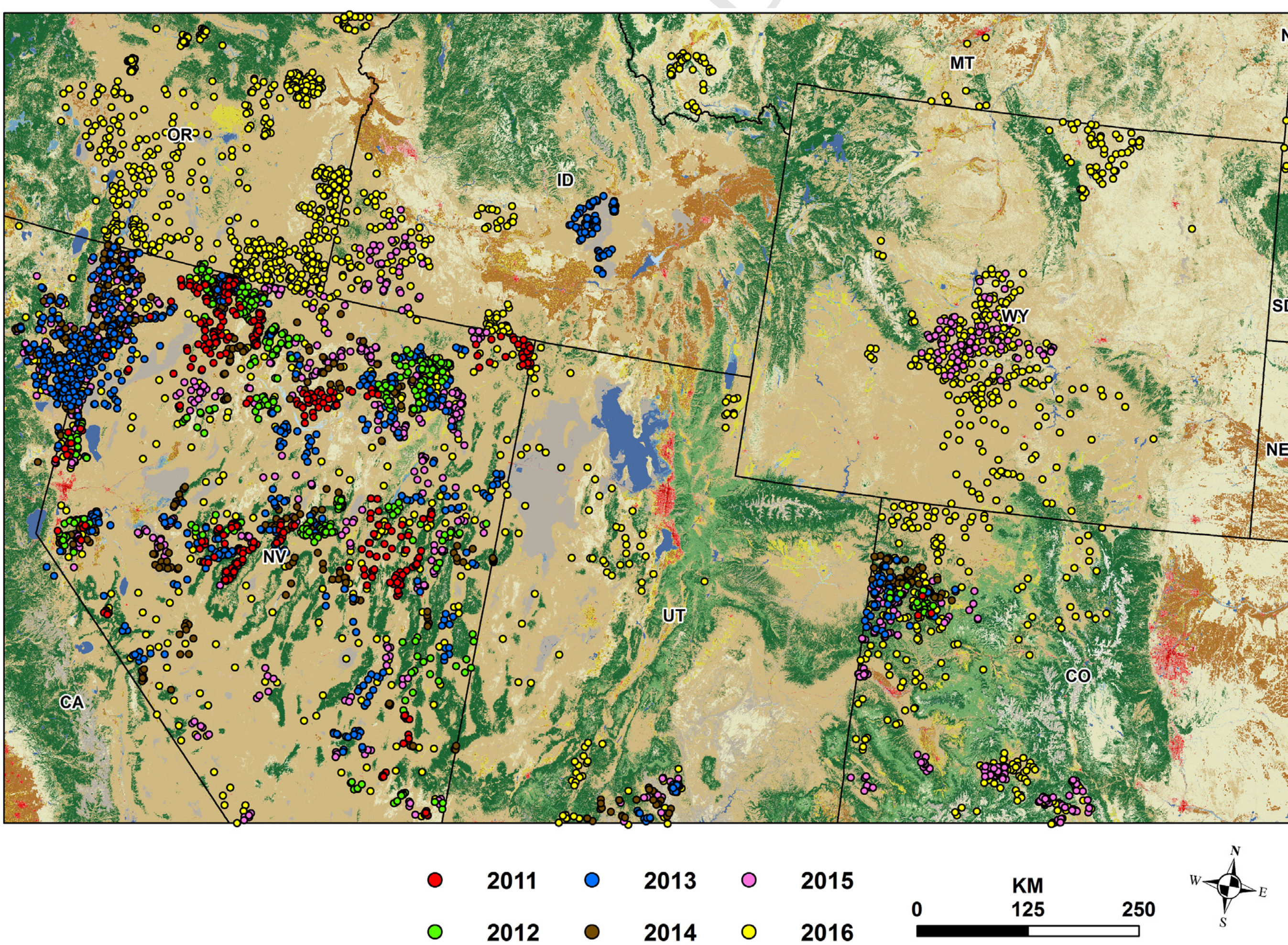

Figure 2. Assessment Inventory and Monitoring (AIM) plot locations delineated temporally by color overlaid on the 2011 National Land Cover Database. We compared AIM data with corresponding mapped estimates of annual grass percent cover to assess the maps' accuracies.

Table 3
Comparing Bureau of Land Management Assessment Inventory and Monitoring (AIM) plots to annual grass—percent cover mapped estimates. The AIM plots represent from 4.5% to 15.2% of a 250-m pixel, depending on the transect length in the plot design. The spatial resolution disparity between datasets likely affects the statistics that describe the relationship. The units are percent based on AIM plot data.

Yr	*r*	MAE (%)	nRMSE (%)	*n* =
2011	0.60	15.69	0.23	332
2012	0.55	14.92	0.19	367
2013	0.39	7.89	0.17	712
2014	0.50	12.15	0.17	569
2015	0.49	12.44	0.20	721
2016	0.50	13.90	0.20	1489
All Yrs	0.50	12.62	0.18	4190

grass percent cover likely was assimilated into other vegetation types' cover at the 250-m pixel scale and diluted as a percentage of the total at that coarser scale. The spatial difference between the 250-m pixels and AIM plots led us to conduct a 3 × 3 standard deviation focal scan on our 2011—2016 maps to identify areas of high variability. We eliminated plots from comparison that fell in areas of high variability, with pixels of high variability defined by exceeding the median value of the focal scan. This allowed us to compare AIM plots to points on our maps where local spatial variability was moderate or low. However, the standard deviation focal scan produced results with severely reduced data ranges, which substantially affected the correlation coefficient and MAE statistics, so we rejected the standard deviation focal scan output. In addition to the spatial resolution challenge, AIM plots can occur anywhere within a 250-m pixel. On the infrequent occasion (< 5%) when the footprint of an AIM plot fell at the intersection of multiple pixels with highly variable estimated values, we removed the plot from the analysis.

Leave-One-Out Validation

Leave-one-out validation is a spatially rigorous assessment technique effective at assessing maps that represent large geographical areas (Wylie et al., 2007; Zhang et al., 2011; Boyte et al., 2018). This technique mitigates spatial autocorrelation by sorting all reference data into 10 spatially and temporally randomly sorted groups and then, systematically, withholding each group as test data and using the remaining 9 groups as training data to develop 10 individual models. For this study, we chose to create 10 groups of reference data (Fig. 3) so that group members were distributed spatially, and the group test datasets were large enough to generate robust model accuracy metrics. To conduct a different analysis, we separated the 30-m annual herbaceous percent cover datasets derived from the high-resolution WorldView data from the 30-m north-central Nevada cheatgrass percent cover and the Owyhee Upland annual grass index data derived from Landsat data. We used the data derived from WorldView scenes once as test data while the data from the two other datasets were used to train the model. We then inverted the test and training datasets and repeated the process. Separating the WorldView-derived data from the north-central Nevada and the Owyhee Upland data before running the model allowed us to understand better the spatiotemporal

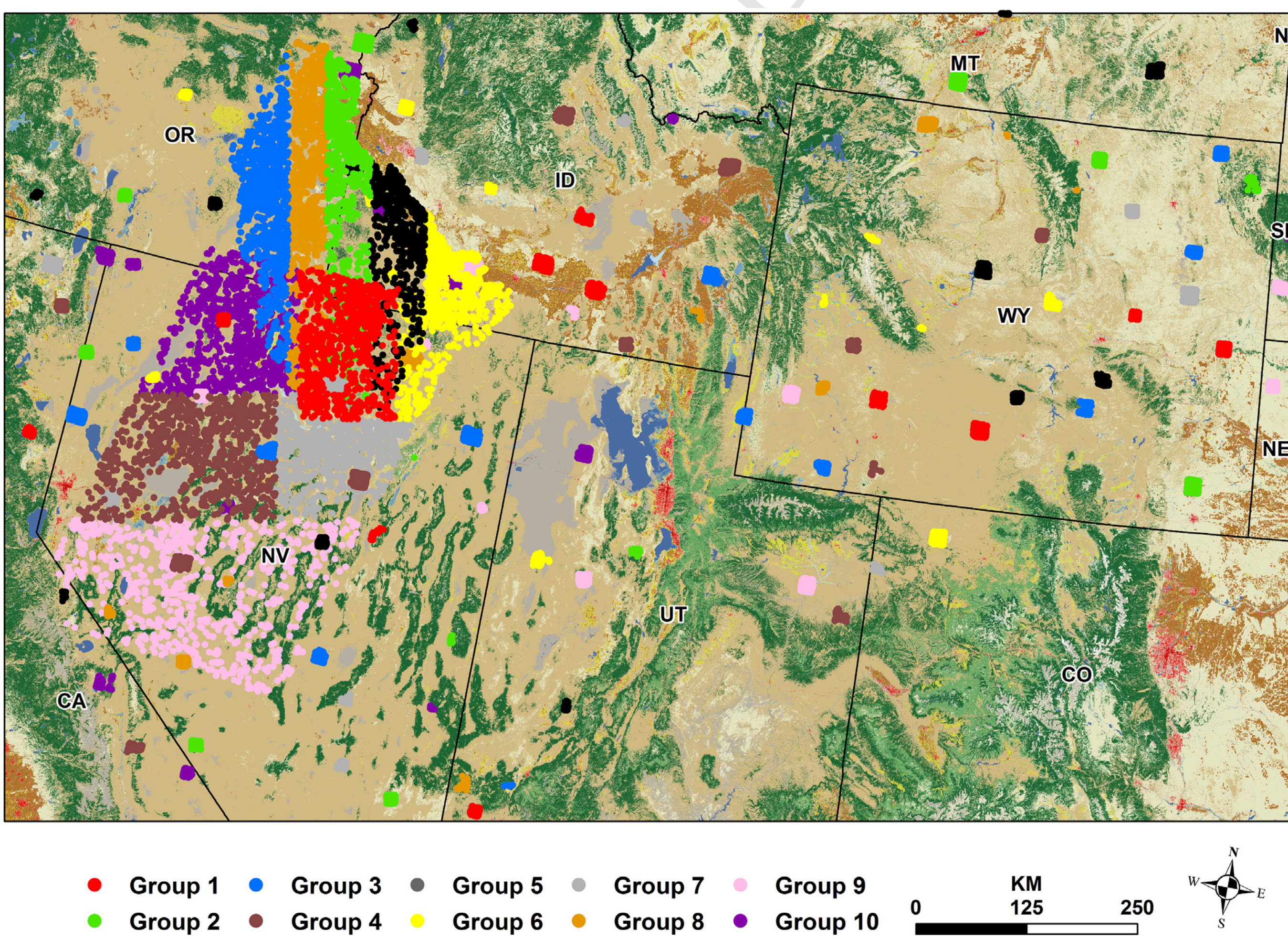

Figure 3. The 10 leave-one-out groups displayed and delineated by color. We randomly sorted the WorldView annual herbaceous vegetation (2013–2015) dataset, north-central Nevada cheatgrass percent cover dataset (~2001), and Owyhee Upland annual grass index (2006) into 10 groups and used them iteratively to evaluate model accuracy.

Table 4
The leave-one-out technique statistics. This technique sorts > 33 000 points from the WorldView, north-central Nevada, and Owyhee Uplands data into 10 random groups. We withheld each group systematically and iteratively as test data and used the remaining nine groups to train the model. In addition, we withheld all WorldView data as test data and used the Nevada and Owyhee Uplands data to train the model. We then inverted this process using the Nevada and Owyhee Uplands data as test data and the WorldView data to train the model.

Group	Test *r*	Test MAE (%)	Test nRMSE (%)	Range	Test *n* =
1	0.48	10.41	0.15	0-99	3960
2	0.62	10.85	0.17	0-95	4388
3	0.47	4.93	0.13	0-55	3221
4	0.63	10.45	0.15	0-100	3615
5	0.93	8.14	0.12	0-99	2208
6	0.86	10.01	0.14	0-100	2212
7	0.67	8.20	0.13	0-100	5659
8	0.65	5.70	0.12	0-67	2203
9	0.41	5.31	0.10	0-99	2639
10	0.61	8.01	0.13	0-98	3361
All groups	0.71	8.43	0.13	—	
Peterson test	0.68	16.10	0.18	0-85	9018
WorldView test	0.52	10.59	0.25	0-100	24359

dynamics of these datasets. For each individual model run, the regression-tree software generated a correlation coefficient and an MAE rate, and we calculated the nRMSE (Table 4). The leave-one-out technique evaluated the mapped estimates of annual grass percent cover using 250-m spatial resolution data (i.e., the WorldView-derived data and the north-central Nevada and Owyhee Uplands datasets after they were spatially averaged from 30 m to 250 m). The random sorting of the dependent variable datasets generated groups that were both spatially and temporally diverse, which helped mitigate model extrapolation bias.

Quantifying Bias

We quantified bias between the annual grass maps and the leave-one-out validation dataset. The bias was quantified at 5% and 95% cover and determined on the basis of a theoretical minimum and maximum of 0 − 100% cover, which also was the range of the predicted values. For AIM data, we used the regression equation that compared the AIM dataset to mapped estimates of annual grass percent cover (see Eq. (2)) at the values of 5% and 95% cover. It is important to note that because the "any-hit" collection strategy used to gather the AIM data can theoretically lead to data values > 100%, and the sampling strategies used to create the mapped estimates' reference data cannot generate values that exceed 100%, the calculated difference between the estimates of annual grass percent cover and the expected *y*-values does not measure true bias.

$$y = 1.1053x + 5.4649 \quad (3)$$

We used the regression equation from the leave-one-out validation data (see Eq. (1)) that was compared with the mapped estimates of annual grass percent cover. This equation was used to calculate the expected *y*-values at the estimated values of 5% and 95% cover. The difference between the estimates of annual grass percent cover and the expected *y*-values measured bias.

$$y = 0.8975x + 3.549 \quad (4)$$

Results

The model's use of independent variables helps the user understand the variables that most influence model development (see Table 1). Overall, the annual grass − percent cover model uses elevation and the Spring GSN substantially more than other variables. Summer GSN, while seldom used to establish conditions that stratify rules, is used in 93% of the model algorithms, equal to the model's usage of elevation for algorithm development. Other variables the model uses frequently include 30-yr precipitation and available water capacity, a measure of soil water potential. Soil organic matter and SOST contribute relatively infrequently to rules stratification, but the model uses each to develop at least 73% of the algorithms. Topographical variables other than elevation (i.e., north steep slope and south steep slope) are used least by the model and only for algorithm development.

Annual Grass −Percent Cover Model and Maps

The annual grass − percent cover model shows a training and test data R^2 equal to 0.76 and 0.74, respectively (see Table 1). The model also shows a training and test data MAE rate equal to 5.79% with a standard deviation (SD) of ±0.03 and 5.84% with an SD of ±0.11, respectively. The 10-fold cross validation produced an R^2 of 0.74 and an MAE rate of 5.90%. Estimated annual grass − percent cover during the 17-yr time series ranges from 0 to 100 and experiences substantial temporal and spatial variability. We illustrate this variability by displaying the annual grass maps with the two lowest (2002 and 2012) and the two highest (2005 and 2016) overall average percent cover in the time series (Fig. 4; Table 5); (access the time series of data and associated metadata at [dataset] Boyte and Wylie, 2017). The Snake River Plain ecoregion tracks from eastern Idaho through south-central and southwestern Idaho into eastern Oregon, and this ecoregion consistently experiences some of the highest annual grass percent cover in the study area (Fig. 5). The ecoregion's 17-yr mean annual grass percent cover equals 19.88 compared with 7.31 for the entire study area, and 88% of pixels that average > 60% throughout the study period are located here. This high percent cover mapping consistency is further illustrated by the coefficient of variation map, which shows relatively low variability in much of this area. In northern Nevada and southeast Oregon, 2 yr—2005 and 2016—stand out as especially prolific for annual grass percent cover, with values exceeding 70% in select places during both yr (see Fig. 4). Examining the time series mean map and recognizing that the coefficient of variation map shows relatively substantial variability in these areas indicates that these 2 yr are likely outliers. In northern Nevada during 2012, our model estimated anomalously low annual grass percent cover following a productive 2011 (see Table 5). A relatively substantial annual grass percent cover exists throughout much of the study period in northeast Colorado, northwest Nebraska, and southeast Wyoming, but overall cover in this area only occasionally exceeds 30%. Thus, the most heavily invaded areas are northern Nevada and the Snake River Plain, although the middle of these two areas, at the intersection of Nevada, Idaho, and Oregon, exhibits low annual grass percent cover throughout the time series.

The annual grass percent cover datasets are each positively skewed with substantially more low percent cover values than high percent cover values. This is evident from the time series' median values and narrow 25th percentile and 75th percentile ranges while every yr's data range (≥ 99) is much broader (Fig. 6A). Table 5 also demonstrates the temporal variability of annual grass percent cover where the overall mean percent cover ranges from 6.14 in 2012 to 11.25 in 2016. Departures from the 17-yr normal percent cover for the study period range from 16% lower than average (2012) to 54% higher than average (2016). Over large geographical areas, average interannual variability in annual grass percent cover is strongly driven by weather, especially precipitation (Bradley and Mustard, 2005; Pilliod et al., 2017), including timing and seasonal totals (Boyte et al., 2016). Figure 6A and B illustrates how estimated annual grass percent cover and seasonal precipitation (defined as October–May) track throughout the time series (we did not use seasonal or annual precipitation to model annual grass percent cover.). For most years, annual grass − percent cover patterns track closely with seasonal precipitation. Deviations from the normal pattern exist during 2001 and 2007 when less-than-average precipitation

Please cite this article as: Boyte, S.P., et al., Validating a Time Series of Annual Grass Percent Cover in the Sagebrush Ecosystem, (2018), https://doi.org/10.1016/j.rama.2018.09.004

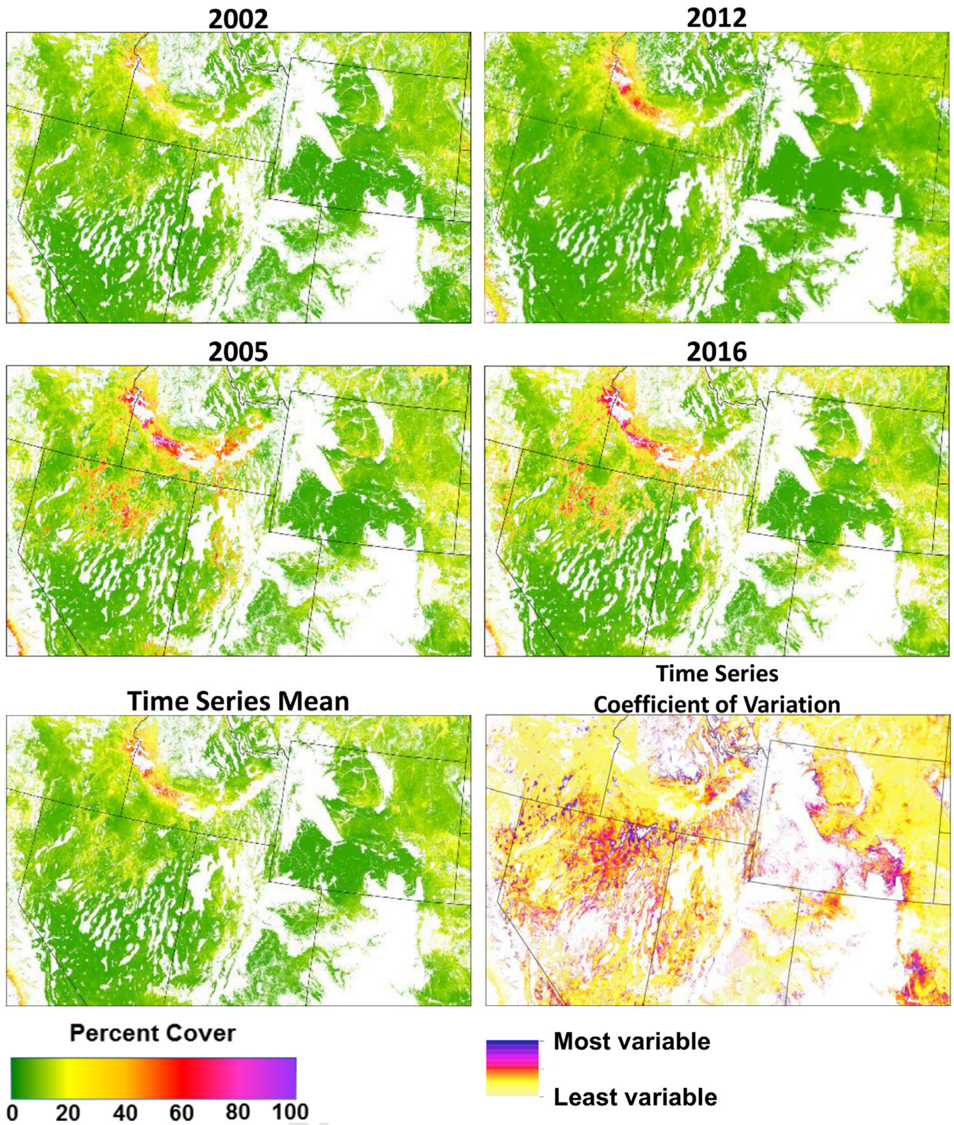

Figure 4. We spatially contrast the 2 yr with the overall lowest percent cover (2002 and 2012) with the 2 yr with the overall highest percent cover (2005 and 2016). These maps are an example of the temporal variability of annual grass percent cover through the 17-yr time series. Percent cover varies annually based on disturbances, management, and weather, especially precipitation. We also show the 17-yr percent cover mean and the coefficient of variation maps. The mask (white) covers areas not classified as shrub or grassland/herbaceous by the National Land Cover Database or areas at or above 2 250-m elevation.

corresponds with slightly more-than-average annual grass percent cover. Also in 2008 and 2009, average and slightly less-than-average precipitation correspond with less-than-average annual grass percent cover. Substantial peaks in annual grass percent cover during 2005 and 2011 correspond with substantial peaks in seasonal precipitation. The final 3 yr of the time series show progressively increasing precipitation totals and progressively increasing annual grass percent cover. This includes the highest annual grass-percent cover value of the time series in 2016.

Model Evaluation

Despite the substantial spatial resolution differences between datasets, a comparison of 6 yr of BLM AIM data with corresponding annual grass — percent cover maps shows moderately strong agreement for most years. With the range of yearly AIM data values being highly variable, the correlation coefficient is marginally effective in describing the relationship between the datasets, so we focus on the MAE rate and nRMSE (see Table 3). We also quantified the difference at the values of 5% and 95% cover, generally, between the AIM data and the corresponding annual grass — percent cover maps for all years combined. The MAE rates vary widely, with the highest rate registered in 2011 at 15.60% and the lowest rate registered in 2013 at 7.89%. The nRMSE ranges from 0.17 in 2013 and 2014 to 0.23 in 2011. When we combine all 6 yr of data, the MAE rate is 12.62% and the nRMSE is 0.18. Figure 7 shows the comparison between AIM data and modeled estimates of annual grass percent cover. The scatterplot reveals an abundance of points in the bottom left corner, a scarcity of points in the lower right corner, and few data points above 40% on the x-axis. Many of the more substantial differences between datasets could be related to differences in the spatial footprints of the AIM data and annual grass — percent cover maps because variability in vegetation is likely to be higher over the larger footprints of the maps' pixels. Overall, the data regression line shows relative consistency with the 1:1 line. There is a fairly consistent underestimation by the annual grass — percent cover maps, which could be related to lower canopy hits in the AIM data. Higher cover values than what exist in the WorldView, north-central Nevada, and Owyhee Uplands data would result from the "any-hit" method. At an estimated cover of 5%, the expected y-value equaled 10.99% cover based on the regression equation (Eq. (3)). At an

Please cite this article as: Boyte, S.P., et al., Validating a Time Series of Annual Grass Percent Cover in the Sagebrush Ecosystem, (2018), https://doi.org/10.1016/j.rama.2018.09.004

Table 5
Statistics describing the 17-yr time series of annual grass — percent cover estimates in the sagebrush ecosystem. The data distribution is skewed positive; therefore, the mean percent statistic is more sensitive than the median to high percent cover. Statistics are calculated only on unmasked areas where the National Land Cover Database classifies a pixel as shrub or grassland/herbaceous and the elevation is at or below 2 250 m.

Yr	Mean percent cover	Change from 17-yr mean percent cover	% change from 17-yr mean percent cover	Range
2000	7.38	0.07	0.96	0-99
2001	7.63	0.32	4.38	0-100
2002	6.34	−0.97	−13.27	0-100
2003	7.33	0.02	0.27	0-100
2004	7.15	−0.16	−2.19	0-100
2005	10.60	3.29	45.01	0-100
2006	7.42	0.11	1.50	0-100
2007	8.08	0.77	10.53	0-100
2008	6.52	−0.79	−10.81	0-100
2009	6.49	−0.82	−11.22	0-100
2010	7.70	0.39	5.34	0-100
2011	8.67	1.36	18.60	0-100
2012	6.14	−1.17	−16.01	0-100
2013	6.43	−0.88	−12.04	0-99
2014	7.98	0.67	9.17	0-100
2015	8.86	1.55	21.20	0-100
2016	11.25	3.94	53.90	0-100
17-yr mean	7.31	–	–	0-96

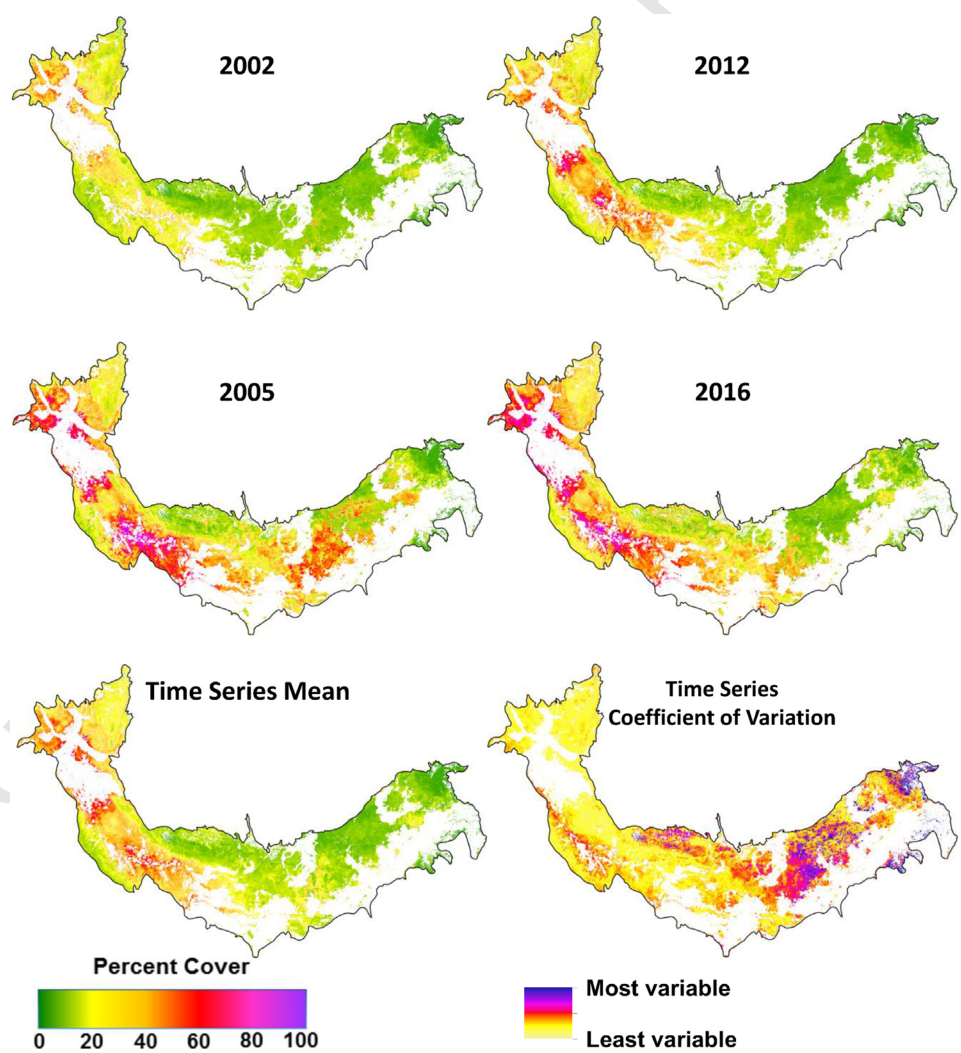

Figure 5. Estimated annual grass — percent cover (**A**) and seasonal (October–May) precipitation (**B**) tracked throughout the study period. The boxes show each yr's median value and 25th and 75th percentiles. Seasonal precipitation totals were more strongly correlated to the temporal variability of estimated annual grass percent cover than were annual precipitation totals. Statistics were derived from data that were masked to areas classified by the National Land Cover Database as shrub or grassland/herbaceous at or below 2 250-m elevation.

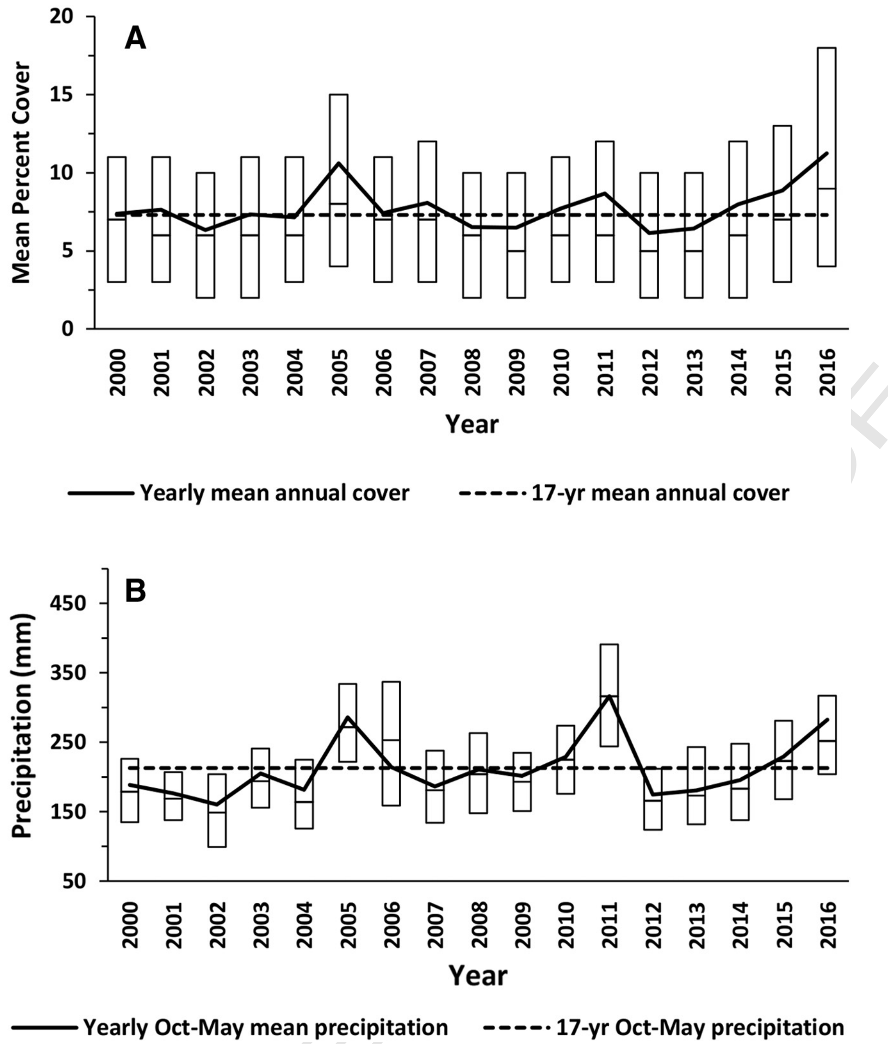

Figure 6. Comparing all yrs of Bureau of Land Management Assessment and Inventory Monitoring data to corresponding yrs of estimated annual grass percent cover.

estimated cover of 95%, the expected y-value equaled 110.47% cover based on the regression equation.

The leave-one-out assessment benefits from spatial resolution agreement between datasets (i.e., both the reference data and mapped estimates of annual grass percent cover) represent a 250-m footprint. For the 10 randomly sorted groups, the lowest $r = 0.41$ and the highest $r = 0.93$ (see Table 4). The MAE rate ranges from 4.93% to 10.85%. Combining data from the 10 groups renders an r of 0.71 and an MAE rate of 8.43%. To conduct a different analysis, we separated the WorldView reference data from the north-central Nevada and Owyhee Uplands reference data. We used the WorldView reference data as test data, developing the model using only the north-central Nevada and Owyhee Uplands data. The model developed renders a test MAE rate of 10.59 and an nRMSE of 0.18. When the north-central Nevada and Owyhee Uplands data are used as test data, the test MAE rate = 16.10% and nRMSE = 0.25. In the leave-one-out assessment, the location of the regression line in relation to the 1:1 line in Figure 8 demonstrates that the model is most accurate when it estimates about 35% annual grass percent cover. Below that threshold, the model slightly underestimates annual grass percent cover, and above that threshold the model overestimates annual grass percent cover. Quantifying bias in the leave-one-out assessment shows at an estimated cover of 5%, the expected y-value equals 8.04% cover based on the regression equation (see Eq. (4)). At an estimated cover of 95%, the expected y-value equals 88.81% cover.

Discussion

The invasion of annual grasses in the sagebrush ecosystem poses challenges to land managers, scientists, and practitioners because these grasses alter historical fire regimes, making fires more frequent, larger, and more severe (Whisenant, 1990; Balch et al., 2013). The changed fire regime adds to the continued degradation of the sagebrush ecosystem and requires these constituent groups to respond differently to new ecological realities. Even fighting fires has become potentially more dangerous as highly flammable grasses invade open meadows and scablands, land covers that formerly served as safe zones for firefighters (Kerns et al., 2016a, 2016b). The current study develops a synoptic annual grass—percent cover model and associated maps in the sagebrush ecosystem for a 17-yr period, and this time series constitutes the longest consistent annual grass-mapping project over the broadest geographical area in the sagebrush ecosystem of which we are aware. The map results support the assertion that annual grasses are spatially variable because of site conditions (Chambers et al., 2016), even over multiple ecoregions. The map results also support the assertion that precipitation is a strong driver of annual grass percent cover (Bradley and Mustard, 2005; Pilliod et al., 2017). An increasing trend in both seasonal precipitation totals and annual grass percent cover is evident since 2012, although the timing of precipitation could explain deviations from expected patterns of annual grass percent cover to seasonal precipitation totals during earlier years of the time series (see Fig. 6).

Please cite this article as: Boyte, S.P., et al., Validating a Time Series of Annual Grass Percent Cover in the Sagebrush Ecosystem, (2018), https://doi.org/10.1016/j.rama.2018.09.004

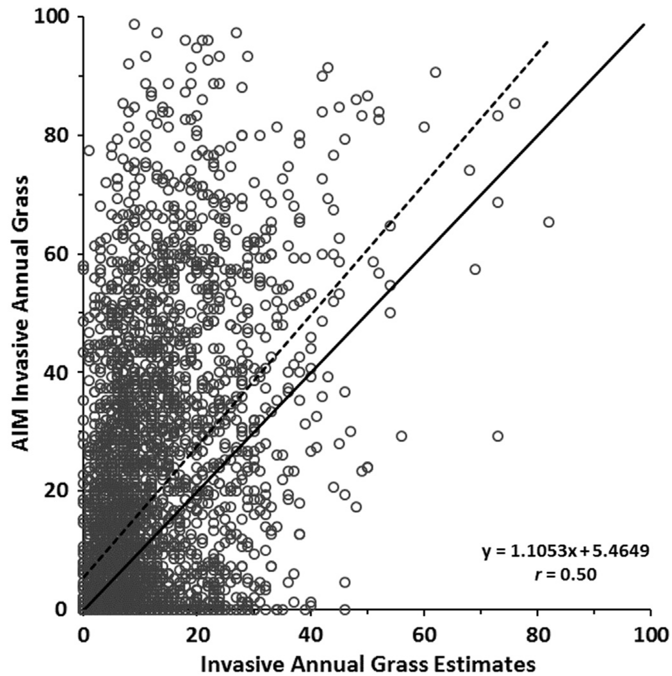

Figure 7. The leave-one-out assessment scatterplot that illustrates the relationship of reference data to annual grass estimates of all 10 randomly sorted groups. The reference data include three spatially explicit datasets—a north-central Nevada cheatgrass percent cover dataset (~2001), an Owyhee Upland annual grass index (2006), and percent cover estimates of annual herbaceous vegetation (2013–2015).

We evaluate the model and maps using two techniques. One evaluation technique employs an approach that uses field-based BLM AIM data. We acknowledge the substantial spatial difference between the AIM data and the 250-m spatial resolution of annual grass — percent cover maps where an AIM plot covers at most 15.2% of a 250-m pixel. However, the multiyear collection strategy, ubiquity, and availability of the AIM data make it a reasonable choice for assessment of the time series, especially as continuous years of available field validation data that spatially match 250-m remote sensing data are extremely uncommon (Browning et al., 2015, 2017; Bradley et al., 2018). Figure 7 illustrates the relationship between data from AIM plots and corresponding estimated annual grass percent cover. Because an AIM plot is much smaller than a pixel of an annual grass — percent cover map, higher values in the AIM data will correspond with lower values in a pixel because species variability is more likely in a broader space. This makes the abundance of points in the upper left corner of the scatterplot foreseeable. The absence of all but one point in the lower right corner of Figure 7 indicates that the annual grass — percent cover model rarely produces high values at a 250-m pixel scale that are associated with low values at the AIM plot scale. This phenomenon occurring frequently would indicate significant model error, so the scarcity of such points helps validate the mapping model.

A second evaluation technique, leave-one-out, is a spatially random approach that mitigates spatial autocorrelation issues and accounts for the expansive geographic territory from where the training data are harvested. The leave-one-out comparison shows a relatively strong agreement between datasets with an overall test MAE rate of 8.43% and an overall test nRMSE of 0.13 (see Table 4). The model generates better prediction test error terms (MAE and nRMSE) when WorldView-derived data are withheld as test data than when the north-central Nevada and Owyhee Uplands data are withheld as test data. This implies that the mapping algorithms developed solely on the Great Basin and Snake River Plain areas are not as robust when they are applied to eastern extents of the study area. This may indicate functional differences between annual grass in the Great Basin and annual grass in Wyoming and Colorado. Certainly, the northeastern and southeastern parts of Wyoming will have significantly greater grass components that will complicate the separation of annual herbaceous vegetation. These east-to-west differences in annual grass — percent cover mapping can also be related to temporal differences because the north-central Nevada and Owyhee Uplands datasets are developed with reference data collected before 2007 while the WorldView datasets are developed with reference data collected after 2012.

Overall, the agreement between the dependent variable and annual grass estimates is relatively strong based on the *r*, MAE error rates, nRMSE, and proximity of the regression lines to the 1:1 lines in Figures 7 and 8. The difference is evident between the regression line and 1:1 line when comparing the AIM data and annual grass maps in Figure 7 and, in many cases, likely related to the spatial resolution and the "any-hit" strategy of the AIM data gathering technique. The "any-hit" effect is likely compounded at higher percent cover, which is reflected in the much higher difference quantified at 95% cover (+15.47%) than at 5% cover (+5.99%). Bias is evident in Figure 8 and demonstrates minor underestimation (−3.04%) at 5% cover, modest overestimation (+6.19%) at 95% cover, and nearly no bias at about 35% annual grass percent cover. The substantially greater number of data points at lower values than higher values in Figure 8 suggests that while annual grass can be present in high percent cover over relatively large areas (250-m pixels), in our mapped time series, low percent cover is much more likely to occur, generally reflecting variability of vegetation, litter, and bare ground components in 250-m pixels. In the leave-one-out approach, no spatial resolution difference occurs between the reference data and modeled data, so the differences between these datasets should be less than with the AIM data comparison.

We hypothesized that the time series of maps would visually exhibit both spatial and interannual variability of annual grass percent cover in already invaded areas and that this interannual variability would closely follow seasonal precipitation patterns. Areas invaded by annual grasses do experience interannual variable percent cover because of spatially dispersed and intermittent disturbances and management activities. However, weather, especially precipitation totals and timing (Bradley, 2009) and recent years' precipitation (Pilliod et al., 2017), contributes to this interannual variability across the entire study area and, therefore, has broader impact. In Figure 6A and B, we see that 2001 and 2007 are

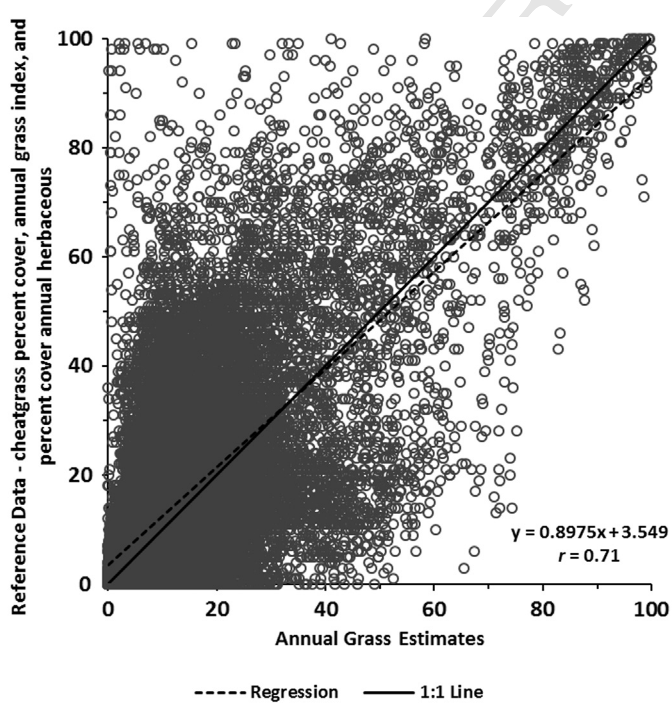

Figure 8.

Please cite this article as: Boyte, S.P., et al., Validating a Time Series of Annual Grass Percent Cover in the Sagebrush Ecosystem, (2018), https://doi.org/10.1016/j.rama.2018.09.004

deviations from the normal mean percent cover/seasonal precipitation pattern when less-than-average seasonal precipitation corresponds with a slight increase in annual grass percent cover. Cheatgrass seeds can stay viable for several years, and Pilliod et al. (2017) discovered that, in the Great Basin, high cheatgrass seed production during 1 yr can lead to high cheatgrass cover in subsequent years if adequate precipitation is received. We do not have data for all 3 yr before 2001, but we do for 2007, and 2005 experienced precipitation 34% above the 17-yr normal and annual grass percent cover 45% above the 17-yr average. We postulate that the effects from 2005 could drive the 2007 annual grass percent cover higher than the 17-yr average even while 2007 precipitation is slightly less than the 17-yr precipitation normal. This assumes that the slightly less than normal precipitation that occurs in 2007 meets the definition of adequate (Pilliod et al., 2017). On a more localized scale, our model estimates anomalously low annual grass percent cover in northern Nevada in 2012 following a highly productive 2011 for this area. This phenomenon is not necessarily unexpected, even though a prolific growing season would leave abundant seed for germination during the subsequent growing season (Kerns and Day, 2017). This is because adequate moisture must be present at the correct time before seeds can germinate. A progressive increase in annual grass percent cover can be observed in northern Nevada from 2013 until 2016 (see Fig. 4). This localized area might serve as a harbinger of high overall percent cover for the entire study area. In 3 of the 4 highest yr of overall annual grass percent cover (see Table 5), this localized area also has its highest annual grass percent cover. In no other year does this geographical area show the level of invasion it does during 2005, 2011, and 2016 (see Fig. 4; Table 5).

Most of the study area shows annual grass percent cover during some, if not all, years in our time series. However, some areas are typically void of substantial annual grass production (e.g., the southwest corner of Wyoming, much of central Nevada, and east-central California). It is likely that these areas possess characteristics that allow them to resist annual grass dominance. Chambers et al. (2016) discusses several environmental characteristics that drive plant community resistance to exotic annual *Brome* grass invasion including elevation, climate, and soils. Our annual grass model's usage of variables converges with these findings where elevation represents the second most heavily used driver (see Table 1), and soil metrics—available water capacity and soil organic matter—and 30-yr precipitation are used heavily as well. Other characteristics can contribute to the resistance of annual grass invasion including the presence of intact biotic soil crusts (Condon and Pyke, 2018), traits of invading plants, interactions between the invaders, native plant communities (Chambers et al., 2014, 2016), and land use history (Pyke et al., 2016).

Implications

Annual grasses in the sagebrush ecosystem present challenges to the responsible use and management of this ecosystem. The more substantial the annual grass domination, the more fire regimes change and increase the severity and frequency of disturbances, and the more difficult it becomes to manage for multiple uses like wildlife habitat, recreation, grazing, and development. Management needs to be able to identify actions that may alleviate the current cycle of invasive annual grass species. The time series of maps developed for this study allows examination of annual grass distribution trends and, through these trends, supports the understanding that annual grass percent cover experiences spatiotemporal variability in this ecosystem for specific reasons. Understanding the drivers of these dynamics provides land managers, scientists, and practitioners with the tools needed to better understand, manage, and use the ecosystem, especially if they understand when and to what degree these drivers are likely to change. The time series allows longitudinal comparisons with temporally dynamic exogenous conditions like weather and grazing. Therefore, correlating annual grass percent cover variability throughout the time series with changing exogenous conditions could help predict future conditions. The time series also allows comparisons with spatially endogenous conditions like topography, soil characteristics, and species competition.

Acknowledgments

Thanks are due to Jennifer Rover for reviewing an earlier version of this manuscript, Thomas Adamson for his proofreading suggestions, and the two anonymous reviewers who gave important feedback that improved this paper. We also thank Steve Hanser, USGS Ecosystems Mission Area program specialist, for serving as the conduit for BLM funds.

References

[Dataset]Boyte, S.P., Wylie, B.K., 2017. A time series of herbaceous annual cover in the sagebrush ecosystem. US Geological Survey—ScienceBase. https://doi.org/10.5066/F71J98QK.
Balch, J.K., Bradley, B.A., D'Antonio, C.M., Gómez-Dans, J., 2013. Introduced annual grass increases regional fire activity across the arid western USA (1980–2009). Global Change Biology 19, 173–183.
Boyte, S.P., Wylie, B.K., Howard, D.M., Dahal, D., Gilmanov, T., 2018. Estimating carbon and showing impacts of drought using satellite data in regression-tree models. International Journal of Remote Sensing 39, 374–398.
Boyte, S.P., Wylie, B.K., Major, D.J., 2015a. Mapping and monitoring cheatgrass dieoff in rangelands of the Northern Great Basin, USA. Rangeland Ecology & Management 68, 18–28.
Boyte, S.P., Wylie, B.K., Major, D.J., 2016. Cheatgrass percent cover change: comparing recent estimates to climate change—driven predictions in the northern Great Basin. Rangeland Ecology & Management 69, 265–279.
Boyte, S.P., Wylie, B.K., Major, D.J., Brown, J.F., 2015b. The integration of geophysical and enhanced Moderate Resolution Imaging Spectroradiometer Normalized Difference Vegetation Index data into a rule-based, piecewise regression-tree model to estimate cheatgrass beginning of spring growth. International Journal of Digital Earth 8, 118–132.
Bradley, B.A., 2009. Regional analysis of the impacts of climate change on cheatgrass invasion shows potential risk and opportunity. Global Changes in Biology 15, 196–208.
Bradley, B.A., Curtis, C.A., Fusco, E.J., Abatzoglou, J.T., Balch, J.K., Dadashi, S., Tuanmu, M.N., 2018. Cheatgrass (*Bromus tectorum*) distribution in the intermountain western United States and its relationship to fire frequency, seasonality, and ignitions. Biological Invasions 20, 1493–1506.
Bradley, B.A., Mustard, J.F., 2005. Identifying land cover variability distinct from land cover change: cheatgrass in the Great Basin. Remote Sensing Environment 94, 204–213.
Brooks, M.L., D'Antonio, C.M., Richardson, D.M., Grace, J.B., Keeley, J.E., DiTomaso, J.M., Hobbs, R.J., Pellant, M., Pyke, D., 2004. Effects of invasive alien plants on fire regimes. Bioscience 54, 677–688.
Browning, D.M., Maynard, J.J., Karl, J.W., Peters, D.C., 2017. Breaks in MODIS time series portend vegetation change: verification using long-term data in an arid grassland ecosystem. Ecology Applications 27, 1677–1693.
Browning, D.M., Rango, A., Karl, J.W., Laney, C.M., Vivoni, E.R., Tweedie, C.E., 2015. Emerging technologies and cultural shifts advancing drylands research and management. Frontiers in Ecology and the Environment 13, 52–60.
Chambers, J.C., Bradley, B.A., Brown, C.S., D'Antonio, C., Germino, M.J., Grace, J.B., Hardegree, S.P., Miller, R.F., Pyke, D.A., 2014. Resilience to stress and disturbance, and resistance to *Bromus tectorum* L. invasion in cold desert shrublands of western North America. Ecosystems 17, 360–375.
Chambers, J.C., Germino, M.J., Belnap, J., Brown, C.S., Schupp, E.W., St. Clair, S.B., 2016. Plant community resistance to invasion by *Bromus* species: the roles of community attributes, *Bromus* interactions with plant communities, and *Bromus* traits. In: Germino, M.J., Chambers, J.C., Brown, C.S. (Eds.), Exotic brome-grasses in arid and semiarid ecosystems of the western U.S.: causes, consequences, and management implications. Springer International Publishing, Cham, Switzerland; Heidelberg, Germany; New York, NY, USA; Dordrecht, The Netherlands; London, England, pp. 275––304.
Commission for Environmental Cooperation, 2009. North American terrestrial ecoregions Level III. Commission on Environmental Cooperation, Montreal, Quebec, Canada.
Condon, L.A., Pyke, D.A., 2018. Fire and grazing influence site resistance to *Bromus tectorum* through their effects on shrub, bunchgrass and biocrust communities in the Great Basin (USA). Ecosystems.
Connelly, J.W., Hagen, C.A., Schroeder, M.A., 2011. Characteristics and dynamics of greater sage-grouse populations. In: Knick, S.T., Connelly, J.W. (Eds.), Greater sage-grouse: ecology and conservation of a landscape species and its habitats. University of California, Berkeley, CA, USA, pp. 53–67.
D'Antonio, C.M., 2000. Fire, plant invasions, and global changes. In: Mooney, H.A., Hobbs, R.J. (Eds.), Invasive species in a changing world. Island Press, Washington, DC, and Covelo, CA, USA, pp. 65––93.
D'Antonio, C.M., Vitousek, P.M., 1992. Biological invasions by exotic grasses, the grass/fire cycle, and global change. Annual Review of Ecology and Systematics 23, 63–87.
French, N.H.F., Bourgeau-Chavez, L.L., Falkowski, M.J., Goetz, S.J., Jenkins, L.K., Camill III, P., Roesler, C.S., Brown, D.G., 2013. Remote sensing for mapping and modeling of land-based carbon flux and storage. In: Brown, D.G., Robinson, D.T., French, N.H.F., Reed, B.C. (Eds.), Land use and the carbon cycle. Cambridge University Press, Cambridge,

England; New York, NY, USA; Melbourne, Australia; Madrid, Spain; Cape Town, South Africa; Singapore; Sao Paulo, Brazil; Delhi, India; and Mexico City, Mexico, pp. 95–143.

Gu, Y., Howard, D.M., Wylie, B.K., Zhang, L., 2012. Mapping carbon flux uncertainty and selecting optimal locations for future flux towers in the Great Plains. Landscape Ecology 27, 319–326.

Gu, Y., Wylie, B.K., Boyte, S.P., Picotte, J., Howard, D.M., Smith, K., Nelson, K.J., 2016. An optimal sample data usage strategy to minimize overfitting and underfitting effects in regression tree models based on remotely-sensed data. Remote Sensing 8.

Herrick, J.E., Van Zee, J.W., McCord, S.E., Courtright, E.M., Karl, J.W., Burkett, L.M., 2017. Monitoring manual for grassland, shrubland, and savanna ecosystems. USDA-ARS Jornada Experimental Range, Las Cruces, NM, USA.

Homer, C.G., Aldridge, C.L., Meyer, D.K., Schell, S.J., 2012. Multi-scale remote sensing sagebrush characterization with regression trees over Wyoming, USA: Laying a foundation for monitoring. International Journal of Applied Earth Observation & Geoinformation 14, 233–244.

Jenkerson, C.B., Maiersperger, T.K., Schmidt, G.L., 2010. eMODIS—a user-friendly data source. US Geological Survey Open-File Report 2010-1055, Reston, VA, USA.

Jensen, J.R., 2005. Introductory digital image processing: a remote sensing perspective. Pearson Prentice Hall, Upper Saddle River, NJ, USA 526 p.

Jung, M., Reichstein, M., Bondeau, A., 2009. Towards global empirical upscaling of FLUXNET eddy covariance observations: validation of a model tree ensemble approach using a biosphere model. Biogeoscience 6, 2001–2013.

Kerns, B.K., Day, M.A., 2017. The importance of disturbance by fire and other abiotic and biotic factors in driving cheatgrass invasion varies based on invasion stage. Biological Invasions 19, 1853–1862.

Kerns, B.K., Zald, H., Krawchuk, M.A., Vaillant, N., Kim, J., Naylor, B.J., 2016a. Ecosystem change in the Blue Mountains ecoregion, funded Joint Fire Science Progam proposal. USDA Forest Service, Pacific Northwest Research Station, Corvallis, OR, USA.

Kerns, B.K., Zald, H., Krawchuk, M.A., Vaillant, N., Kim, J.B., Naylor, B.J., 2016b. Ecosystem change in the Blue Mountains ecoregion: exotic invaders, shifts in fuel structure, and management implications. 7 — 12 August 101st Ecological Society of America Annual Meeting, Fort Lauderdale, FL, USA.

Kokaly, R.F., 2011. DESI—Detection of Early-Season Invasives (software-installation manual and user's guide version 1.0). US Geological Survey Open-File Report 2010-1302, Reston, VA, USA.

Liu, Z., Wimberly, M.C., 2016. Direct and indirect effects of climate change on projected future fire regimes in the western United States. Science Total Environment 542 (Part A), 65– — 75.

Maynard, J.J., Karl, J.W., Browning, D.M., 2016. Effect of spatial image support in detecting long-term vegetation change from satellite time-series. Landscape Ecology 31, 2045–2062.

Peterson, E.B., 2005. Estimating cover of an invasive grass *(Bromus tectorum)* using tobit regression and phenology derived from two dates of Landsat ETM + data. International Journal of Remote Sensing 26, 2491–2507.

Peterson, E.B., 2007. A map of annual grasses in the Owyhee Uplands, Spring 2006, derived from multitemporal Landsat 5 TM imagery. US Department of Interior, Bureau of Land Management, Nevada State Office, Reno, Carson City, NV, USA.

Pilliod, D.S., Welty, J.L., Arkle, R.S., 2017. Refining the cheatgrass-fire cycle in the Great Basin: precipitation timing and fine fuel composition predict wildfire trends. Ecology and Evolution.

Pyke, D.A., Chambers, J.C., Beck, J.L., Brooks, M.L., Mealor, B.A., 2016. Land uses, fire, invasion: exotic annual *Bromus* and human dimensions. In: Germino, M.J., Chambers, J.C., Brown, C.S. (Eds.), Exotic brome grasses in arid and semiarid ecosystems of the western US: causes, consequences, and management implications. Springer International Publishing, Cham, Switzerland; Heidelberg, Germany; New York, NY, USA; Dordrecht, The Netherlands; London, England, pp. 307– — 337.

Schoennagel, T., Balch, J.K., Brenkert-Smith, H., Dennison, P.E., Harvey, B.J., Krawchuk, M.A., Mietkiewicz, N., Morgan, P., Moritz, M.A., Rasker, R., Turner, M.G., Whitlock, C., 2017. Adapt to more wildfire in western North American forests as climate changes. Proceedings of the National Academy of Sciences U S A 114, 4582–4590.

West, N.E., Young, J.A., 2000. Intermountain valleys and lower mountain slopes. In: Barbour, M.G., Billings, D. (Eds.), North American terrestrial vegetation, 2nd ed. Cambridge University Press, Cambridge, United Kingdom, pp. 256–284.

Whisenant, S.G., 1990. Changing fire frequencies on Idaho's Snake River Plains: ecological and management implications. INT-276. USDA, Ogden, UT, USA, pp. 4– — 10.

Wiken, E., Francisco, J.N., Griffith, G.E., 2011. North American Terrestrial Ecoregions—Level III. Commission for Environmental Cooperation, Montreal, Canada.

Wylie, B.K., Boyte, S.P., Major, D.J., 2012. Ecosystem performance monitoring of rangelands by integrating modeling and remote sensing. Rangeland Ecology & Management 65, 241–252.

Wylie, B.K., Fosnight, E.A., Gilmanov, T.G., Frank, A.B., Morgan, J.A., Haferkamp, M.R., Meyers, T.P., 2007. Adaptive data-driven models for estimating carbon fluxes in the northern Great Plains. Remote Sensing Environment 106, 399–413.

Xian, G., Homer, C.G., Rigge, M.B., Shi, H., Meyer, D., 2015. Characterization of shrubland ecosystem components as continuous fields in the northwest United States. Remote Sensing Environment 168, 286–300.

Zhang, L., Wylie, B.K., Ji, L., Gilmanov, T.G., Tieszen, L.L., Howard, D.M., 2011. Upscaling carbon fluxes over the Great Plains grasslands: sinks and sources. Journal of Geophysical Research 116.

Web references

BLM Assessment Inventory and Monitoring (AIM), d. . Available at: https://gis.blm.gov/AIMdownload/layerpackages/BLM_AIM_Terrestrial.lpk, Accessed date: 26 October 2017.

Earth Explorer, d. . Available at: https://earthexplorer.usgs.gov, Accessed date: 27 June 2018.

GDAL, d. . Available at: http://www.gdal.org, Accessed date: 4 April 2013.

Landscape Approach Data Portal, d. . Available at: https://landscape.blm.gov/geoportal/catalog/AIM/AIM.page, Accessed date: 20 April 2018.

Monitoring trends in burn severity, d. . Available at: http://www.mtbs.gov/index.html, Accessed date: 17 April 2017.

Nevada Natural Heritage Program, d. . Available at: http://heritage.nv.gov, Accessed date: 13 April 2017.

The National Land Cover Database, d. . Available at: http://www.mrlc.gov/nlcd2001.php, Accessed date: 3 January 2018.

The National Map, d. . Available at: https://nationalmap.gov/elevation.html, Accessed date: 4 August 2016.

Remote sensing phenology, d. . Available at: http://phenology.cr.usgs.gov/index.php, Accessed date: 13 September 2017.

POLARIS, d. . Available at: http://stream.princeton.edu/POLARIS/, Accessed date: 30 March 2017.

PRISM Climate Group, d. . Available at: http://prism.oregonstate.edu, Accessed date: 27 August 2015.

RuleQuest, d. . Available at: https://www.rulequest.com, Accessed date: 10 September 2015.

AUTHOR QUERY FORM

ELSEVIER	**Journal: RAMA** **Article Number: 341**	**Please e-mail your responses and any corrections to:** **E-mail: corrections.ESI@elsevier.spitech.com**

Dear Author,

Please check your proof carefully and mark all corrections at the appropriate place in the proof (e.g., by using on-screen annotation in the PDF file) or compile them in a separate list. Note: if you opt to annotate the file with software other than Adobe Reader then please also highlight the appropriate place in the PDF file. To ensure fast publication of your paper please return your corrections within 48 hours.

For correction or revision of any artwork, please consult http://www.elsevier.com/artworkinstructions.

We were unable to process your file(s) fully electronically and have proceeded by

☐ Scanning (parts of) your article ☐ Rekeying (parts of) your article ☐ Scanning the artwork

Any queries or remarks that have arisen during the processing of your manuscript are listed below and highlighted by flags in the proof. Click on the 'Q' link to go to the location in the proof.

Location in article	**Query / Remark: click on the Q link to go** **Please insert your reply or correction at the corresponding line in the proof**
Q1	Please provide caption.
Q2	Your article is registered as a regular item and is being processed for inclusion in a regular issue of the journal. If this is NOT correct and your article belongs to a Special Issue/Collection please contact j.beckemeier@elsevier.com immediately prior to returning your corrections.
Q3	The author names have been tagged as given names and surnames (surnames are highlighted in teal color). Please confirm if they have been identified correctly.
Q4	Correctly acknowledging the primary funders and grant IDs of your research is important to ensure compliance with funder policies. We could not find any acknowledgement of funding sources in your text. Is this correct?
Q5	Please provide page range for Gu, Herrick, and Kerns?
Q6	Please provide the volume number and page range for the bibliography in Condon and Pyke, 2018.
Q7	Please provide the volume number and page range for the bibliography in Pilliod et al., 2017.
Q8	For Zhang please provide missing vol or page number. Please check this box if you have no corrections to make to the PDF file. ☐

Thank you for your assistance.